

# Physisorption and Chemisorption of Alkanethiols and Alkyl Sulfides on Au(111)

David J. Lavrich, Sean M. Wetterer, Steven L. Bernasek,\* and Giacinto Scoles\*

*Department of Chemistry and Princeton Materials Institute, Princeton University, Princeton, New Jersey 08544*

*Received: October 31, 1997; In Final Form: February 25, 1998*

The energetics and kinetics of the adsorption of a variety of sulfur-containing hydrocarbons onto Au(111) have been explored using helium beam reflectivity and temperature-programmed desorption (TPD) techniques. Simple alkanethiols as well as dialkyl sulfides, dialkyl disulfides, and other sulfur-containing organics were found to adsorb with a low coverage physisorption enthalpy about 20% greater than the heat of vaporization in the bulk. In contrast to the dialkyl sulfides that only physisorb, alkanethiols and dialkyl disulfides also interact chemically with the gold with a chemisorption enthalpy of 126 kJ/mol that is independent of alkyl chain length. The presence of sterically hindering substituent groups on the carbon atom adjacent to the sulfur atom produces, however, a reduction in the chemisorption enthalpy of up to 15%. Temperature-programmed desorption of nonequilibrated, high exposure layers of alkanethiols with eight carbon atoms or longer displayed a second, higher energy, chemisorption peak at 148 kJ/mol which could be eliminated by annealing, leaving only the lower energy chemisorption peak. The chemisorption rate of molecules in the physisorbed precursor state has also been measured. Arrhenius plots for the chemisorption of a series of alkanethiols from their physisorbed precursors show that the chemisorption activation energy is 28.8 kJ/mol and is independent of chain length.

## 1. Introduction

Self-assembled monolayers (SAMs) have been the subject of much recent research because they provide an opportunity to systematically modify the composition and properties of solid surfaces, and as a consequence, they are projected to be technologically important.<sup>1–6</sup> Among the many SAM systems that have been investigated, those made by adsorbing alkanethiols on single-crystal gold surfaces have been more frequently studied because of their ease of preparation, range of functionalities, and excellent stability.<sup>7</sup> The principal ingredient for obtaining self-assembly is a relatively strong interfacial binding asymmetry of the molecular constituents. In the alkanethiol SAM case, this is provided by the sulfur affinity for gold, and a comparably strong lateral interaction (4–8 kJ/mol per CH<sub>2</sub>),<sup>8</sup> arising from the van der Waals forces between the chains. This lateral interaction can be controlled by changing the length of the hydrocarbon. While the lateral interactions are relatively well-known, the sulfur–gold interaction in the alkanethiol–gold SAMs has remained the subject of frequent debate. Since a better understanding of headgroup/substrate interactions is essential for any progress in the understanding of the structure and growth kinetics of SAMs, we have embarked on a program to produce accurate measurements of the energetics of the interaction of alkanethiols, dialkyl sulfides, and dialkyl disulfides with the (111) face of single-crystal gold.

SAM formation was thought, until recently, to proceed via simple Langmuir-type kinetics.<sup>9</sup> However, the recent discovery of the existence of a lower density phase (the so-called striped phase)<sup>10</sup> and an extensive series of adsorption experiments (carried out with LEED,<sup>11</sup> STM,<sup>12</sup> X-ray and atomic beam scattering<sup>13,14</sup>) have made clear that SAM growth from the vapor occurs in at least two steps. Atomic force microscopy (AFM)<sup>15</sup> studies have recently shown this is also true when the growth

occurs from solution. Furthermore, in gas-phase deposition, the impingement rate (pressure) dependence of the growth rate appears to follow a complex behavior with evidence for a linear, quadratic, and saturated growth regime,<sup>16</sup> making a better knowledge of the different adsorption energies essential to any progress in understanding this complex problem. Only a few data on adsorption energies are available in the literature. On the basis of the adsorption of hexane, Nuzzo<sup>17</sup> has predicted a methylene–surface interaction of 8 kJ/mol. He has also reported an energy of 117 kJ/mol for dimethyl disulfide adsorption as methyl thiolate.

The fact that alkanethiols can both physisorb through van der Waals interactions which can be changed by varying the chain length and chemisorb through the sulfur bond provides an excellent opportunity to study the role of the physisorbed precursor state in the chemisorption kinetics. Furthermore, several other interesting questions can be posed. For instance, is the chemisorption energy a function of the chain length? What desorption behavior can be expected for a molecule that, because of the length of its alkane chain, has a physisorption energy higher than the chemisorption energy? How much do these energies change in the case of disulfides or because of the presence of substituents on the hydrocarbon chain located at different distances from the chemisorbing thiol group? By posing and, in most cases, answering these questions, this paper provides a simpler and more unified picture of the interaction of this important class of molecules with an extremely widely used, but only partially understood, substrate.

## 2. Experimental Section

The instrument designed to conduct the experiments is based on an ultrahigh-vacuum (UHV) scattering chamber capable of reaching and maintaining a vacuum of  $1 \times 10^{-10}$  Torr. In the center of this chamber is a sample manipulator with six degrees of freedom, equipped with a 40 W heater and liquid nitrogen

\* To whom correspondence should be addressed.

cooling so that sample temperatures in the range 125–1000 K can be achieved. Mounted on the manipulator is a gold crystal cut to expose its (111) face. Positioned in the chamber at  $45^\circ$  to the gold surface normal and 10 cm from the surface is an Extrel quadrupole mass spectrometer. In the same plane on an axis normal to the mass spectrometer axis is the He beam line. The supersonic He beam source (20 mm diameter, 1 MPa pressure) creates at the surface a beam of approximately  $1 \times 10^{14}$  molecules/(s cm<sup>2</sup>). The nozzle is located at 45.7 cm from the surface in a chamber that is pumped by a 4000 L/s VHS-250 diffusion pump. After passing a 0.5 mm skimmer, the He beam is twice differentially pumped and collimated by two 3 mm holes at 10 cm separation. The beam is chopped at a frequency of 340 Hz with a 50% duty cycle. The Au(111) crystal is typically cleaned by Ar<sup>+</sup> bombardment for 15 min followed by annealing at 850 K for at least 15 min.

The basic experiment consists of reflecting the helium beam from the gold surface and into the mass spectrometer which is tuned to 4 *m/e*. A clean gold surface will reflect up to about 30% of the impinging helium beam. The presence of adsorbates on the surface causes an increase in the diffuse scattering of the helium beam which decreases the specular intensity. The adsorbates are introduced by leaking the molecules into the UHV chamber while the pressure is monitored by an ionization gauge. As molecules stick to the gold surface, the specular intensity drops in relation to the concentration and ordering of the adsorbates on the surface. The sensitivity to ordering arises from the fact that the diffuse scattering cross section of an isolated molecule is substantially larger than the area occupied by a molecule in a two-dimensionally condensed island. Island formation thus produces a higher specular reflectivity than that produced by random adsorption.

The general technique used here to explore the energetics of adsorbate binding was temperature-programmed desorption (TPD). The experiments consisted of leaking a sample into the UHV chamber while the Au(111) surface was held at a constant temperature, usually low enough that the sticking coefficient of the molecules was unity. The molecules adsorbed onto the surface until the He beam specularity was mainly due to diffuse scattering (about 4% of the maximum specularity). The gold crystal was then heated at approximately 2 K/s while the specular intensity was monitored. As adsorbates desorbed, the specular intensity increased in relation to the amount of gold exposed. The rate of specular increase is maximum near the temperature of maximum desorption. The temperature of maximum desorption is used with the Redhead<sup>18</sup> equation to estimate the enthalpy of desorption.

Temperature-programmed desorption is a well-established technique, but it has been used only rarely with specular helium scattering as a probe of surface coverage.<sup>19</sup> Figure 1 shows typical TPD data obtained in the apparatus. In this example, hexanethiol was deposited onto a clean Au(111) surface at 200 K. The surface was then heated while the He specularity was monitored. The solid line in the upper trace in Figure 1a exhibits the He specularity as a function of the recorded sample temperature. At two different temperatures there is a rapid increase in specularity. The final increase in specularity is followed by a decrease due to increased inelastic scattering (Debye–Waller attenuation).<sup>20</sup> The experimentally determined Debye–Waller attenuation on the bare gold is shown in the upper trace as the dashed line. The solid curve is corrected for this Debye–Waller attenuation and then differentiated to yield the trace in part b of Figure 1. For sake of comparison, the dashed curve in Figure 1b shows the result of differentiating

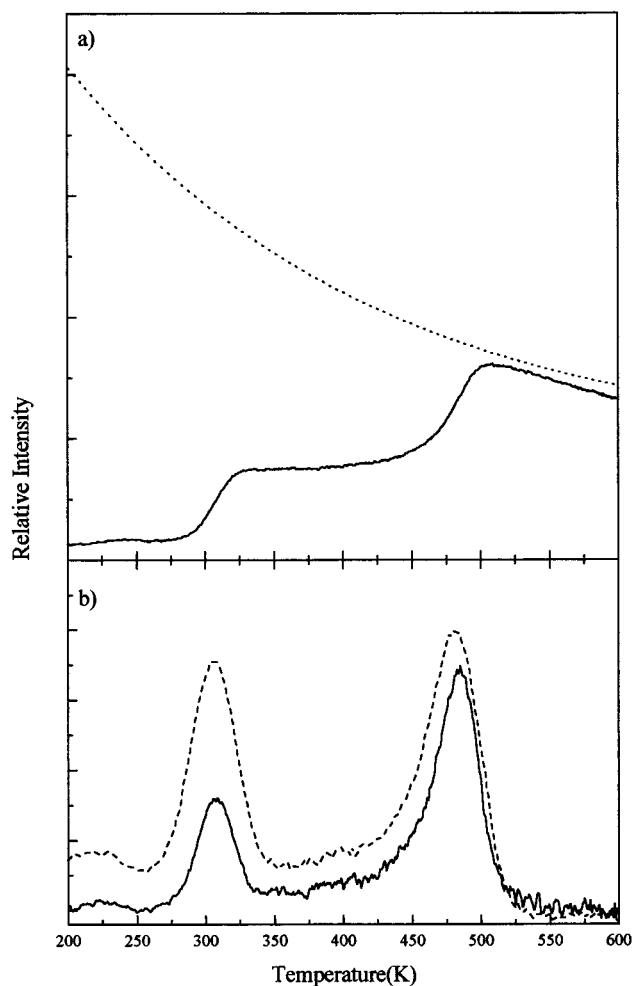


**Figure 1.** Temperature-programmed desorption of hexanethiol adsorbed on Au(111). The dotted line in (a) is the Debye–Waller attenuation due to the clean gold surface. The solid line in (a) is the raw He beam specularity as the gold temperature is ramped (after deposition of the thiol) from 200 to 600 K at an average rate of 2 K/s. In (b) the first derivative of the data is displayed, before and after they have been corrected for Debye–Waller attenuation.

the data of Figure 1a without correcting for the Debye–Waller effect. While peak positions are essentially unaffected by the correction, peak intensities may be affected. The peaks of the corrected curve were fit to Gaussian forms using standard nonlinear least-squares fitting routines as a means of obtaining peak locations and peak widths. The first is located at  $305 \pm 3$  K with a full width at half-maximum (fwhm) of  $28.1 \pm 0.3$  K. The second peak occurs at  $480 \pm 5$  K with a fwhm of  $28.7 \pm 0.2$  K. By assuming a preexponential factor of  $1 \times 10^{13}$  s<sup>-1</sup> and using the Redhead equation with heating rates of 1.9 and 1.5 K/s, respectively (determined from the differential of the experimental heating curve of the sample at the peak temperatures), enthalpies of 79 and 124 kJ/mol for the two desorption peaks were determined. It was found from multiple runs of the same sample that the typical error in peak location between experiments was  $\pm 8$  K, suggesting an error of 2 kJ/mol for the enthalpies. Throughout this paper, discussion will center on the enthalpies of desorption determined as described above.

In a more typical TPD experiment, a mass spectrometer is used to monitor a particular mass of the desorbing species. As the sample is heated, molecules desorb and are detected by the mass spectrometer. The advantages of He reflectivity detected TPD are greater sensitivity and greater surface specificity, while the main advantage of mass spectrometry detected TPD is the

TABLE 1

molecule	energy (kJ/mol)					
	phys	hindered	chem 1	chem 2	phys (calc)	deviation, %
methanethiol	48, 58 <sup>22</sup>				49	2
ethanethiol	57		127		55.1	-3.4
butanethiol	68		127		67.3	-1
hexanethiol	79		124		79.5	0.6
octanethiol	87		125	147	91.7	5.4
nonanethiol	103		127	152	97.8	-5.3
decane			126	146		
dodecanethiol			127			
tetradecanethiol			128			
hexadecanethiol	150				140.5	-6.7
octadecanethiol	158 ± 10				152.7	-3.4
docosanethiol	169 ± 10				177.1	4.8
diethyl sulfide	68				67.3	-1.0
dibutyl sulfide	86				91.7	6.6
diethyl disulfide			124			
<i>tert</i> -butanethiol	64	107			64.5 <sup>a</sup>	0.8
2-propanethiol	64	107			64.5 <sup>a</sup>	
neopentanethiol	68		128	141	70.6 <sup>a</sup>	3.8
thiophene	60				61.5	2.5
1,4-butanedithiol	82	117				
2,3-butanedithiol	80	107	133			
1,6-hexanedithiol			129	150		

<sup>a</sup> Due to the nonlinear and nonplanar nature of the molecules, we have included in the calculations only those atomic groups which may be found to be in direct contact with the surface.

ability to identify the desorbed species. As surface specularity can be affected by the spatial rearrangement of the adsorbates on the surface (e.g., island formation), their presence should be monitored when carrying out measurements of the type reported here.

### 3. Results and Discussion: Energetics

**3.1. Energetics of Alkanethiol Adsorption.** Thermal desorption measurements were carried out for several alkanethiols (ethanethiol, butanethiol, hexanethiol, octanethiol, and nonanethiol) adsorbed at 200 K on the Au(111) surface. In each case, two thermal desorption peaks are observed with data similar to that of Figure 1. As in previous work on the adsorption of alkanes and 1-alkenes,<sup>21</sup> it was found that the peak desorption temperature for the lower temperature peak increased with increasing chain length. The results are summarized in Table 1 and plotted in Figure 2a as a function of the bulk heat of vaporization of the adsorbate. The open circles represent the enthalpy of desorption of the alkanethiols while the filled squares represent alkanes. Both series of data display a similar linear relationship between the two quantities with a slope of 1.15. This relationship implies that the interaction with the surface is also due to van der Waals forces which are responsible for the cohesive energy in the bulk phases. The robustness of the relationship of the physisorption enthalpy to the bulk heat of vaporization is displayed in Figure 2b. Here, a wide variety of molecules ranging from simple alkanes to sulfur-containing alkanes of variable structural complexity, as well as some aromatic compounds, show the same linear relationship between the bulk heat of vaporization of the molecule and its enthalpy of physisorption on the Au(111) surface.

Table 1 displays all the data collected for all the systems studied. The column labeled "phys" indicates energies obtained from peaks assigned to the physisorbed layer, "hindered" indicates a "lower than normal" energy state which is not observed for the linear alkanethiols, "chem 1" refers to the first peak arising from chemisorption which has been identified as the "normal" chemisorption state of the thiols, and "chem 2"

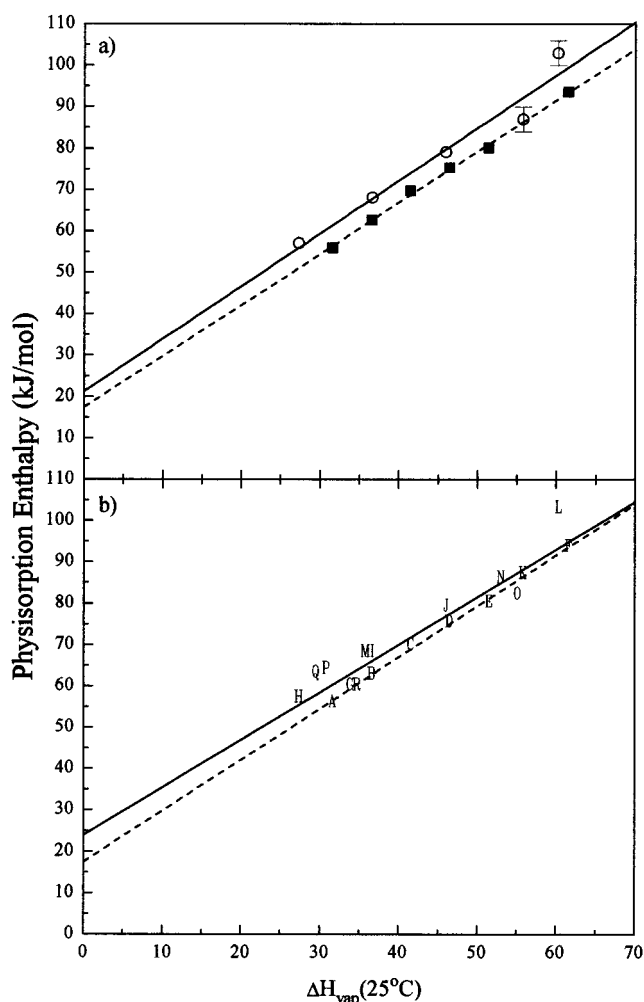


**Figure 2.** (a) Enthalpy of desorption of both alkanethiols (○) and alkanes (■) from Au(111) surfaces plotted against their respective bulk heats of vaporization. The alkanethiols shown are ethanethiol, butanethiol, hexanethiol, and nonanethiol. The alkanes displayed are hexane, heptane, octane, nonane, decane, and dodecane. (b) Enthalpy of desorption of alkanes and various alkanethiols versus their respective bulk heats of vaporization. The compounds presented are (A) hexane, (B) heptane, (C) octane, (D) nonane, (E) decane, (F) dodecane, (G) benzene, (H) ethanethiol, (I) butanethiol, (J) hexanethiol, (K) octanethiol, (L) nonanethiol, (M) diethyl sulfide, (N) dibutyl sulfide, (O) 1,4-butanedithiol, (P) *tert*-butanethiol, (Q) isopropanethiol, and (R) thiophene. The solid line in (a) is a linear fit to the alkanethiol data. The dotted line is a linear fit to the alkane data. In (b), the solid line is a linear fit to all the data, and the dotted line is reproduced from the dotted line in (a) for comparison.

are peaks from a higher energy chemisorption feature that can only be obtained at high coverages and that can be annealed away. The labels "phys(calc)" and "deviation" represent the physisorption energy calculated by theory outlined later in this paper and the difference with experimental results, respectively. Each feature will be discussed in more detail in what follows.

**3.2. Physisorption Enthalpies.** Figure 3 displays the enthalpies of desorption of *all* the features found in the TPD spectra of the alkanethiols plotted as a function of the chain length. The dashed line is a fit to the alkane data established in a parallel study.<sup>21</sup> The open circles represent the physisorption enthalpies for the alkanethiols, with a linear fit of the data displayed as a solid line.

It is not surprising that the slopes of the linear fits to the alkanethiol and alkane physisorption enthalpies are similar because of the relationships with the bulk heats of vaporization

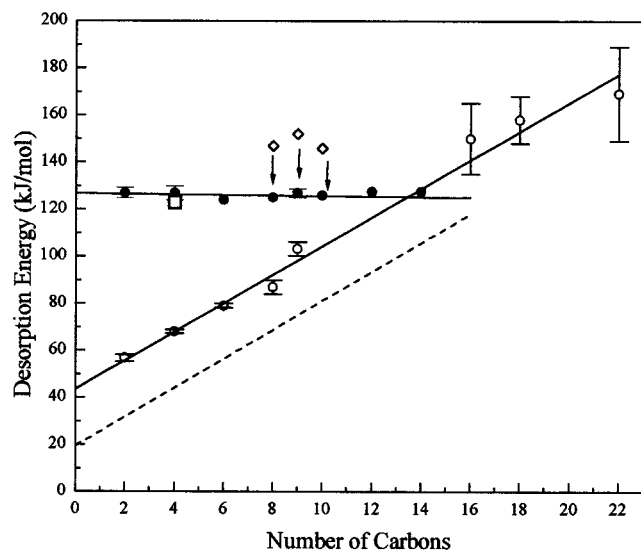


**Figure 3.** Plot of desorption enthalpy versus number of carbons for alkanethiols and alkanes. Desorption enthalpy of alkanethiols from the physisorbed state are shown as (○) and from the chemisorbed state as (●). Solid lines are the result of linear fits to the data. The dashed line is a linear fit to the alkane data from ref 21. (□) Desorption energy of diethyl disulfide.

previously pointed out. These fits are given in the equations below:

$$\Delta H_{\text{Au}}^t = 6.08(0.74) \text{ kJ/mol}(C) + 43.5(5) \text{ kJ/mol}$$

$$\Delta H_{\text{Au}}^a = 6.16(0.16) \text{ kJ/mol}(C) + 19.4(1.4) \text{ kJ/mol}$$

where  $C$  is the number of carbon atoms,  $\Delta H_{\text{Au}}^t$  is the desorption enthalpy of the alkanethiols, and  $\Delta H_{\text{Au}}^a$  is the desorption enthalpy for the alkanes. The difference in offset between the two lines is 24.1 kJ/mol. The linear slope indicates the additive nature of the contribution due to the methylene subunit to the desorption enthalpy, implying that the molecules lie parallel to the metal surface, each unit contributing via its polarizability. The  $\text{CH}_2$  contribution had previously been estimated by Dubois et al.<sup>6,22</sup> as 7.9 kJ/mol. Furthermore, for methanethiol physisorbed on Au(111) Dubois et al. reported adsorption energies of 48.5 and 58 kJ/mol. The presence of the lower energy peak was attributed to multilayering. The linear fit in Figure 3 predicts that methanethiol would physisorb with 51 kJ/mol enthalpy, in good agreement with Dubois et al. It is interesting to note that a study by Sexton and Hughes<sup>23</sup> comparing alcohols, ethers, and alkanes on Cu(100) and Pt(111) showed that a  $\text{CH}_2$  group contributes 5–6.5 kJ/mol on both metals, and the oxygen lone pair contributes 42 kJ/mol on Pt and 35 kJ/mol on Cu.

A parallel study<sup>21</sup> has established that the contributions to the physisorption energy of hydrocarbons on Au(111) can be broken down into additive contributions of atoms or groups of atoms. In particular, a  $\text{CH}_2$  group contributes  $6.2 \pm 0.1$  kJ/mol in a linear chain but 8.1 kJ/mol in cyclic compounds while the  $\text{CH}_3$  groups contribute 15.5 kJ/mol to the physisorption energy. Finally, the additional contribution of a double bond was found to amount to 6.1 kJ/mol. Because of the linear relationship between the heat of adsorption and the chain length, using the above information to extract the contribution of the SH group, the values reported in Table 1 for the linear chains can be predicted. Simple arithmetic assigns to each SH group the value:

$$SH = S + \text{CH}_3 - \text{CH}_2$$

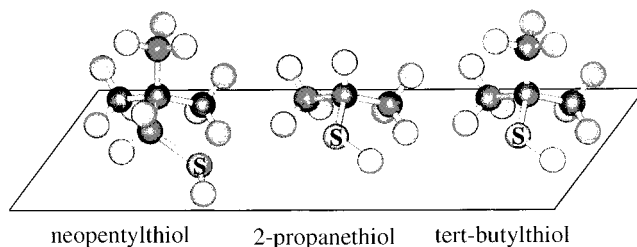


**Figure 4.** Sketch of possible orientation of neopentylthiol, 2-propanethiol, and *tert*-butylthiol physisorbed on Au(111) surface. Only those groups closest to the surface contribute to binding. The dark spheres represent carbon atoms, the lighter spheres represent hydrogen atoms, and the spheres with "S" inscribed are sulfur atoms.

where  $S = 24.1$  kJ/mol is the difference between the y-axis intercepts of the thiol and hydrocarbon lines and  $\text{CH}_3$  and  $\text{CH}_2$  are the contributions of the  $\text{CH}_3$  and  $\text{CH}_2$  groups reported above. This gives for the SH contribution the value 33.5 kJ/mol and the expected good agreement between the calculated and measured values of  $\Delta H$  for the linear chains shown in Table 1. More interesting is the fact that using the same input the adsorption energies of dialkyl sulfides and thiophene can be predicted. Indeed, since  $S$  represents the contribution of an S atom (when added to the chain without altering the number of  $\text{CH}_3$  groups), its value (24.1 kJ/mol) can be used to calculate the value  $\Delta H$  for these molecules. As shown in Table 1, the predicted values ("phys(calc)") agree quite well with the experimental results. A bit more difficult but equally interesting is the possibility to rationalize the experimental adsorption energies of the three nonplanar thiols reported in Table 1. Excellent agreement is obtained also in those cases if only the contributions of the groups that, in the most favorable configuration, can come in direct contact with the surface (see Figure 4) are included.

Finally, it should be pointed out that the adsorption energies for the dithiols cannot be understood in the simple terms reported above. Hexanedithiol chemisorbs so rapidly that a value for  $\Delta H_{\text{phys}}$  could not be obtained for it. The two butanedithiols physisorb (and chemisorb) with energies that are smaller than expected. However, while the chemisorption "anomaly" can be rationalized (discussed later), the low values for the physisorption energy remain (also because of lack of data) unexplained.

**3.3. Chemisorption Enthalpy.** Figure 3 also displays (filled circles) the enthalpy of desorption derived from the second feature in the TPD spectra of alkanethiols ("chem 1" in Table 1). For this feature the enthalpy of desorption does not change with chain length and has an average value of  $126 \pm 2$  kJ/mol. Since binding in all likelihood occurs through the S atoms,<sup>24</sup> the length of the chain would not be expected to play a large role in the desorption enthalpy of the chemisorbed molecules.

At high coverages the adsorption of alkanethiols on Au(111) leads to a well-ordered SAM where the energy for desorption was found previously to be between 126 and 146 kJ/mol.<sup>25</sup> This value is the same for both alkanethiols and dialkyl disulfides. Indeed, dimethyl disulfide has been reported to desorb from Au(111) as a disulfide with an energy of approximately 117 kJ/mol.<sup>17</sup> The average enthalpy for the chain length independent feature in Figure 3 ( $126 \pm 2$  kJ/mol) is completely consistent with this value.

In the present TPD measurements it was observed that the alkanethiols exhibit both a physisorption and a chemisorption feature up to  $n = 8$ . For octanethiol and longer chain thiols, the physisorption feature becomes difficult to detect with TPD, and a third, higher energy peak becomes apparent at  $148 \pm 3$

kJ/mol, which is 21 kJ/mol greater than the desorption energy of the first chemisorption peak (see below under the section "Higher Energy Chemisorption"). The disappearance of the physisorption feature between 100 and 126 kJ/mol is due to the kinetics of chemisorption. For the long-chain thiols the desorption temperature of the physisorbed molecule is high. As the temperature is ramped, the molecules will remain on the surface at temperatures at which the activation barrier to chemisorption can be easily crossed. The chemisorption channel will then compete successfully with the physisorption desorption channel, and the molecules will not be detected to desorb from their physisorbed state.

**3.4. Physisorption vs Chemisorption.** An interesting effect appears as a consequence of the increase in physisorption enthalpy with increased chain length. As shown in Figure 3, the physisorption enthalpy can become larger than the chemisorption enthalpy at chain lengths greater than  $C_{14}H_{30}$ . Data for hexadecanethiol adsorption indicate that the trend continues since the desorption enthalpy for this molecule was measured to be  $150 \pm 15$  kJ/mol. Nuzzo et al. determined that hexadecanethiol desorbs from gold with a desorption enthalpy of approximately 167 kJ/mol.<sup>24</sup> This energy was higher than the "normal thiolate" energy of 117 kJ/mol<sup>17</sup> and was explained by Nuzzo as being caused by a stabilization through interchain interactions. Within the present context, interchain attraction does not need to be invoked to justify the increased value of the desorption energy since the continuation of the physisorption trend for the shorter chains predicts that for a chain of this length the molecules can still be bound to the surface at temperatures where the "chemical" S–Au bond is already broken. Furthermore, at the temperature where hexadecanethiol desorbs ( $>500$  K), it is highly unlikely that the island which forms the compact monolayer will still be stable. At these temperatures the molecules are expected to desorb from an uncondensed two-dimensional gas state since the energy needed for the molecules to detach themselves from the island borders is lower than that needed to desorb from the gold.

To confirm this trend, experiments were performed with longer chain lengths. However, because of the low vapor pressure of hexadecanethiol, octadecanethiol, and docosanethiol, the experiments were carried out with a modified procedure. The gold crystal was cleaned as usual. The UHV sample chamber was vented to nitrogen, and a solution of one of the thiols in ethanol was placed on the gold surface. The machine was pumped down, and TPD was carried out as usual. The TPD peaks were not as sharply defined but clearly showed a desorption energy that continued to increase with chain length, as shown in Figure 3.

**3.5. Higher Energy Chemisorption.** The appearance of the third high-energy peak at  $148 \pm 3$  kJ/mol (shown in Table 1 in the column "chem 2" and as open diamonds in Figure 3) was unexpected. This peak occurs under nonequilibrium growth conditions when the surface has been saturated at high fluxes and low surface temperatures. To clarify its origin, several experiments were conducted by dosing the gold surface with decanethiol at 298 K and then waiting for an amount of time before carrying out the TPD. Figure 5 shows the results of three experiments ranging from no anneal time to 900 s of anneal time to finally 3600 s of anneal time. In this series of spectra, it can be seen that the higher energy peak is largest with no anneal and consistently becomes smaller with longer anneal time. After possibly going through an intermediate state, the normal chemisorption feature becomes larger at the expense of the higher energy peaks, implying that the higher energy

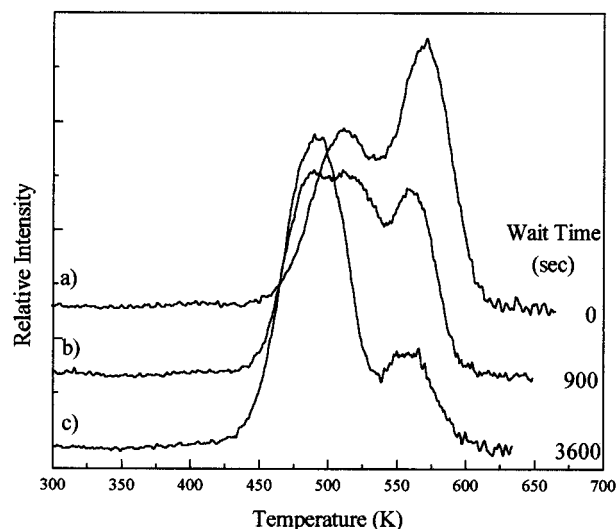


**Figure 5.** Temperature-programmed desorption spectra of decanethiol annealing experiments. A layer of decanethiol on Au(111) is annealed at 343 K for (a) 0, (b) 900, and (c) 3600 s. The higher energy peak (143 kJ/mol) anneals into the lower energy peak (124 kJ/mol).

population anneals into the lower energy state. This is surprising since it is the reverse of what is expected and commonly observed.

A possible explanation that would account for this apparent contradiction is that the higher energy peak is due to desorption as a thiol and the lower energy peak is desorption as a disulfide. Both thiol and disulfide desorption have been reported by Knoll.<sup>26</sup> A comparison of Seller's<sup>27</sup> calculation of methanethiol adsorption on Au(111) with a Born–Haber calculation of desorption as a dimethyl disulfide indicates that desorption as a disulfide is energetically favorable. Under a high flux dosing condition, there may be enough hydrogen present on the surface to facilitate the desorption of thiols. After annealing (or under slower growth conditions) the hydrogen would desorb, leaving only the disulfide desorption channel. A second, and perhaps more likely, explanation can be derived on the basis of a recent STM study of methanethiol adsorption from the gas phase onto clean reconstructed Au(111) by Feher et al.<sup>28</sup> In that paper the authors show that "the dosing rate affects the final structure of the monolayer." At high dosing rates a very large number of regularly spaced islands of vacancies are formed which only upon annealing merge by Ostwald ripening into large depressions while the monolayer (both in and out of the depressions) assumes the normal  $c(4 \times 2)$  structure. If one makes the reasonable assumption that before and after the annealing (which involves motion of the gold atoms on the surface) the binding energy of the S atoms to the gold is different, the present results can then be easily explained.

The fact that the higher energy desorption peak is observed only for chains with more than eight carbons can be explained in the context outlined above. Indeed, as the annealing rate of the chemisorbed phase must be a function of the chain length, both dimerization and gold reorganization rates for chains shorter than eight carbons may be fast enough to allow the annealing to be completed during the temperature ramping of the TPD procedure and before the desorption temperature is reached.

**3.6. Steric Hindrance Effects.** In an attempt to gain further information on the bonding of thiols to the gold surface, other related molecules were studied for comparative purposes. To address the question of disulfide formation, sterically hindered thiol groups were chosen with the hypothesis in mind that if dimer formation was not possible, the binding energy with the

surface would be higher. The TPD spectrum of *tert*-butanethiol (with thiol group attached to a tertiary carbon) showed a low-energy *physisorption* peak consistent with the bulk correlation (see above) and a second feature which, contrary to the stated hypothesis, was at a lower energy (107 kJ/mol). No feature around 124 kJ/mol was found in either case.

Neopentylthiol (a thiol group attached to a primary carbon with a *tert*-butyl end) showed instead a "normal" chemisorption feature at 128 kJ/mol. Although S–H bond strengths differ slightly (368 kJ/mol for ethanethiol and 364 kJ/mol for *tert*-butanethiol),<sup>29</sup> the primary factor responsible for the decreased binding energy of the tertiary and secondary thiols is more likely that sterically hindered thiols are not able to bind as closely to the surface. Steric hindrance quickly ceases to be a factor when an additional methylene unit (as in neopentylthiol) allows the S atom to interact more strongly with the metal surface without forcing other aliphatic groups to do the same, avoiding in this way an increase in the repulsive part of the potential. The extra repulsive energy due to the sterically hindering group is 20 kJ/mol (or approximately 16% of the desorption energy) and will produce a relatively small change in the position (height) of the sulfur atom on the gold surface.

**3.7. Dialkyl Disulfides and Dialkyl Sulfides.** Another set of experiments explored the behavior of diethyl disulfide. TPD indicated the presence of only one desorption peak for diethyl disulfide at 124 kJ/mol (shown as the open square in Figure 3). At first inspection it may appear surprising that no desorption peak corresponding to physisorption was found for this species, since its enthalpy of physisorption should be similar to butanethiol, owing to the similar bulk heat of vaporization. However, the kinetics of chemisorption of the disulfide species are different than for the thiols (see below). Indeed, Dubois et al.<sup>6</sup> found that the sticking probability for dimethyl disulfide was orders of magnitude larger than for methanethiol. They suggested that, for the shorter chain species, the S–S bond was more efficiently cleaved and that disulfides did not exhibit the same activation barrier for adsorption as the thiols. This is not surprising since the overall thermodynamics of chemisorption of thiols involves breakage of the S–H bond as well as formation of the H–Au bonds, H–H bonds, and other reaction pathways. Disulfide chemisorption occurs from a process that requires only cleavage of the S–S bond and formation of two thiolate–gold bonds. According to Fenter et al.,<sup>30</sup> disulfides could chemisorb as dimers without dissociation.

In a final set of experiments the dialkyl sulfides (diethyl sulfide and dibutyl sulfide) were studied to investigate the probability of cleaving the C–S bond. Both compounds showed physisorption enthalpies consistent with the correlation with the bulk heat of vaporization. Neither, however, showed a chemisorption feature. These findings are in apparent contradiction to those of Porter<sup>31</sup> that, under electrochemical conditions, showed C–S bond cleavage in several organosulfides. Other studies, however, support the present findings. In an earlier study utilizing dialkyl sulfides, Troughton et al.<sup>32</sup> found that dialkyl sulfides formed a poorly organized layer from solution. They found that the poor quality of the layer was not due to the decomposition of the dialkyl sulfide, but rather to the fact that the adsorbates were only weakly bonded through the sulfur group. A recent study by Reinhoudt et al.<sup>33</sup> has also shown that a variety of dialkyl sulfides remain intact on the surface and experience no C–S bond cleavage.

Thiophene, a heterocyclic molecule containing four carbon atoms and a sulfur atom, also showed only a physisorption feature for adsorption on gold as in the case of the dialkyl

sulfides. The single desorption peak occurs at 60 kJ/mol, which is consistent with desorption from a physisorbed layer (see above). No other desorption peaks were found, even for samples prepared under high dosing and/or long annealing procedures. No chemisorption features were observed. The thiophene measurements were stimulated by a recent paper of Hemminger<sup>34</sup> and collaborators in which the formation of well-ordered thiophene monolayers on Au(111) was observed. The present work confirms the theoretical results of Elfeninat et al.,<sup>35</sup> who had concluded that thiophene could not chemisorb on Au(111) surfaces.

## 4. Results and Discussion: Kinetics

**4.1. Precursor-Mediated Chemisorption: A Brief Introduction.** Physisorbed precursor states have been investigated with respect to their effect on chemisorption kinetics<sup>36,37</sup> and the dynamics of adsorption and desorption.<sup>38</sup> Typically, in the presence of a direct chemisorption process, sticking coefficients increase with increased surface temperature. Systems that show a decrease in sticking coefficient with increased surface temperature are thought to involve a precursor state.<sup>39–42</sup> The precursor is typically a more weakly bound state such as a physisorbed state. The decrease in sticking coefficient into the chemisorbed state arises from a kinetic competition between desorption from the precursor state and crossing an activation barrier to chemisorption. Precursor chemisorption has been found, for example, for such systems as O<sub>2</sub> on Pt(111),<sup>43</sup> CO and CO<sub>2</sub> on Ni(100),<sup>44,45</sup> and N<sub>2</sub> on W(100).<sup>46</sup> These systems have been explored using molecular beam deposition, studying the dependence of the sticking on the angle of incidence of the molecular beam with the surface, the kinetic energy of the beam, and the surface temperature. Larger molecules have not been as extensively studied with the exception of alkanes on transition metals.<sup>47–52</sup> In these systems, a decrease in initial sticking coefficient has been observed with increasing incident energy and increasing surface temperature.

The gold/alkanethiol system with its relatively low chemisorption energy and physisorption dependence on chain length affords the opportunity to probe the phenomenon of precursor-mediated chemisorption in a way not possible with the diatomic systems. Since only the sulfur headgroup binds with the gold surface with an energy that does not depend on chain length, the chemisorption well remains constant for different chain lengths. Increasing the alkane chain length, however, increases the physisorption (precursor) well depth. In this way, the activation barrier to chemisorption from the physisorbed state can be systematically varied and the process of precursor-mediated chemisorption probed. The basic question that can be asked becomes, is the barrier between the two wells independent of the chain length or does the deepening of the physical attraction decrease the barrier to chemisorption? Since the physisorption interaction is distributed throughout the molecule while the chemisorption well is localized, the first hypothesis is the most probable one. However, the conclusion is not as obvious as to make an experimental verification completely unnecessary.

**4.2. Chemisorption from a Physisorbed Layer.** The use of helium beam specularly to measure chemisorption sticking coefficients is made difficult by the presence of physisorption. Therefore, determining chemisorption sticking coefficients versus surface temperature is not possible other than at temperatures well above the physisorption desorption temperature. However, by using TPD, it is possible to determine whether there is chemisorption from the physisorbed state.

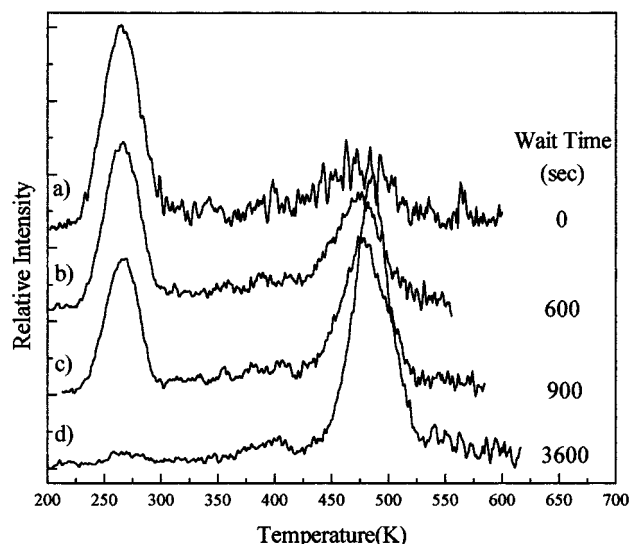


**Figure 6.** Temperature-programmed desorption spectra of a butanethiol layer on Au(111) deposited and "annealed" at 208 K for (a) 0, (b) 600, (c) 900, and (d) 3600 s. The higher energy peak (chemisorbed) becomes more intense over time at the expense of the lower energy peak (physisorbed).

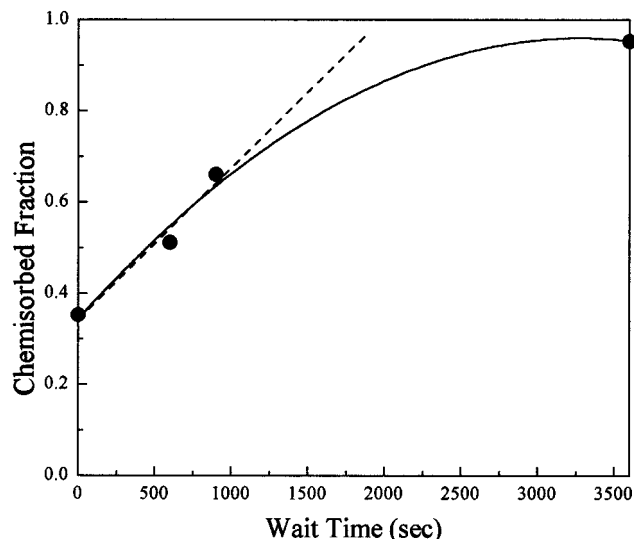


**Figure 7.** Plot showing the chemisorbed fraction of total peak area from Figure 6 as a function of waiting time.

By exposing the surface to adsorbates until a prespecified coverage is reached and then waiting different periods of time before conducting the TPD experiment, the amount of physisorbed species can be compared to the quantity of chemisorbed species. In this series of experiments, it is assumed that the total area of all the peaks in a TPD spectrum is the same irrespective of the physisorbed or chemisorbed status of the molecules that produce the specularly drop. This assumption is probably not strictly correct, but for the present purpose of comparison of similar conditions this should not represent a serious problem.

Figure 6 shows a series of TPD experiments for butanethiol deposited onto a 208 K Au(111) crystal. Curve a shows mostly physisorbed species when the waiting time is zero. A series of curves b, c, and d represent progressively longer waiting times, showing conversion of the physisorbed species into chemisorbed species. The final curve d annealed for 3600 s exhibits mostly chemisorbed species. Figure 7 displays the ratio of chemisorbed peak area to total peak area derived from each of the TPD

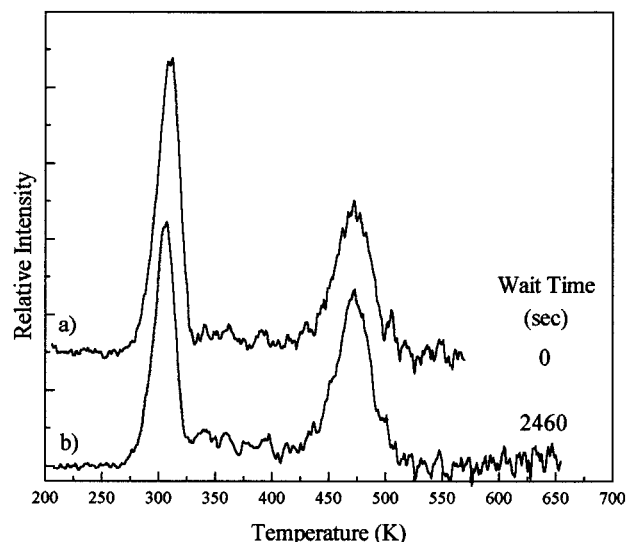


**Figure 8.** Temperature-programmed desorption spectra of hexanethiol layer deposited at 213 K after a waiting time of (a) 0 and (b) 2460 s. The relative intensity of lower energy peak (physisorbed) and higher energy peak (chemisorbed) remain relatively unchanged in this range of waiting time.

profiles in Figure 6. The data clearly show that conversion into chemisorbed species increases with waiting time. The slope of the first three points at shorter waiting times indicates that, at the temperature of  $T = 208$  K, the rate of chemisorption is on the order of  $4 \times 10^{-4} \text{ s}^{-1}$ .

The TPD profiles in Figure 6 show that the physisorption peak location does not change with decreasing coverage but that the chemisorption peak location shifts to higher temperatures with increasing coverage. Annealing at higher temperatures (see above) would be needed to ensure that the gold surface has also equilibrated after chemisorption has occurred. Therefore, no conclusions can be drawn from the presence of these small shifts, but they are noted for the sake of completeness.

The final point in Figure 7 at 3600 s indicates the limit of full conversion into a chemisorbed layer. The y-intercept of 0.35 is a result of the fact that even for no waiting time, there is conversion as the surface temperature is ramped to high temperature. As the surface temperature increases, there is faster chemisorption, and therefore some fraction of physisorbed molecules become chemisorbed during the TPD process even when the waiting time is nominally zero.

Hexanethiol was deposited on Au(111) at 208 K in a similar set of experiments. Once again, the TPD curve obtained after zero waiting time (displayed in part a of Figure 8) shows the presence of both physisorbed and chemisorbed species. Unlike butanethiol, however, after waiting for 2460 s, there appears to be no further conversion to the chemisorbed state. Examining the increase in peak area of the chemisorbed peak from no anneal to 2460 s indicates a growth rate of about  $10^{-5} \text{ s}^{-1}$ . This reduction in chemisorption rate compared to butanethiol could be due either to a change in the activation barrier from the physisorbed to the chemisorbed state or a change in the preexponential factor. This question is considered in the next section.

**4.3. Chemisorption from a Steady-State Physisorbed Population.** A more convenient experiment is to study the growth of the chemisorbed layer in real time at a constant temperature and with a constant physisorbed population on the surface. However, since under these conditions there is a chance that direct chemisorption may contribute to the chemisorption rate, this effect must be taken into account.

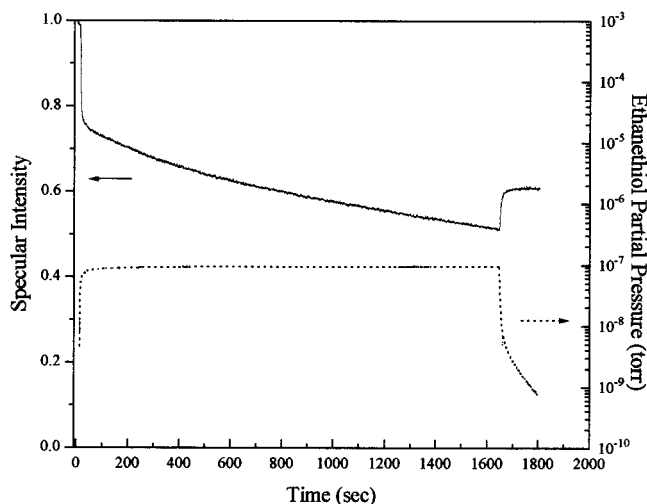


**Figure 9.** Specular decay of Au(111) caused by adsorption of ethanethiol from the gas phase at a surface temperature of 223 K. The solid curve is the raw helium specular signal. The dotted line depicts the partial pressure of ethanethiol in the UHV sample chamber.

By conducting growth experiments in a temperature regime high enough that the desorption rate of the physisorbed molecules is significant (approximately 20 K below the peak physisorption desorption temperature), a steady state of physisorbed molecules can be achieved. Following the simple Langmuir approximation

$$\theta_{ss} = k_a / (k_a + k_d)$$

where  $\theta_{ss}$  is the steady-state coverage of adsorbates,  $k_a$  is the adsorption rate (controlled in part by the partial pressure of the adsorbing molecules), and  $k_d$  is the desorption rate (controlled by the surface temperature). As shown in Figure 9, the specular intensity initially drops to a finite value (0.75) when exposed to a constant flux of molecules which corresponds to a steady-state coverage of physisorbed molecules. However, even though the partial pressure of thiols remains constant for 1600 s, a slower decrease in specular intensity is observed. This is attributed to conversion of the physisorbed molecules into chemisorbed species, thereby “permanently” occupying a fraction of the surface sites and decreasing the fraction of surface available to the physisorption equilibrium. At the end of the growth experiment, the thiols are evacuated from the chamber, and a rapid partial recovery of specular intensity is found. The rate of recovery is consistent with desorption of the physisorbed species. The chemisorption rate is identified as the rate of the slower specular decay and is determined by differentiating this portion of the decay curve and normalizing to the coverage. By conducting this same type of experiment over a range of temperatures, an Arrhenius plot for the physisorption to chemisorption conversion process can be constructed.

Figure 10 shows these Arrhenius plots for ethanethiol, butanethiol, hexanethiol, and decanethiol. For all four species, the same slope is found with different y-intercepts, as shown in Table 2. Since the rates found from the TPD “annealing” experiment in the previous section fall within the data on this Arrhenius plot, it is verified that any direct process contribution is small compared to the precursor-mediated chemisorption.

While the slopes of the Arrhenius plots have sizable errors, they are all within 5% of 29 kJ/mol, independent of chain length. Nuzzo<sup>6</sup> had estimated the barrier to chemisorption of methanethiol from the gas phase as 25 kJ/mol. However, his model predicts that the activation barrier would decrease with chain

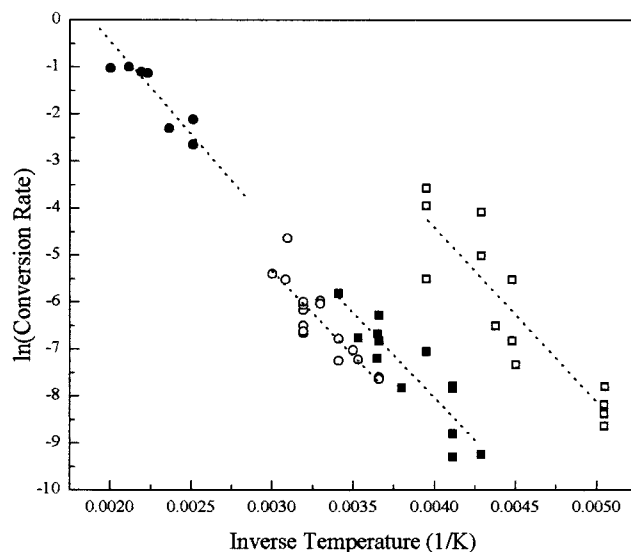


**Figure 10.** Arrhenius plot of the chemisorption rate from a steady-state physisorbed population for ethanethiol ( $\square$ ), butanethiol ( $\blacksquare$ ), hexanethiol ( $\circ$ ), and decanethiol ( $\bullet$ ).

**TABLE 2**

	ethanethiol	butanethiol	hexanethiol	decanethiol
slope (kJ/mol)	$31.0 \pm 4.7$	$29.0 \pm 4.7$	$29.6 \pm 4.4$	$27.3 \pm 5.8$
y-intercept ( $\ln(s^{-1})$ )	$10.5 \pm 2.5$	$6.0 \pm 2.2$	$5.3 \pm 1.8$	$5.9 \pm 1.6$

length. This is due to the fact the chemisorption well for all alkanethiol chain lengths remains fixed, and the physisorbed well becomes deeper with increased chain length. In his model, the transition state is viewed as being stabilized by attractive dispersion forces to a degree comparable to that reflected by the increased heats of adsorption of the molecular precursors.<sup>6</sup> Therefore, increased chain length should decrease the activation barrier. Within the limits imposed by the errors, the present data suggest that while the physisorbed well depth increases the location of the curve crossing with the chemisorbed state remains the same, and therefore the activation barrier to chemisorption remains constant with increasing chain length.

In this model of fixed activation barrier, the rate of chemisorption is controlled in part by the lifetime of the precursor state. Therefore, the overall rate of chemisorption is a branching ratio between chemisorption of the physisorbed molecules and their desorption. With a fixed activation barrier, the rate for chemisorption increases overall with increased surface temperature. The fact that physisorbed TPD features become difficult to detect above chain lengths greater than octanethiol is consistent with this model, since the longer chains remain on the surface at higher temperatures resulting in faster chemisorption.

The mechanism for the “bottleneck” to chemisorption is difficult to ascertain. Typically, for diffusion-controlled processes on surfaces, the activation barrier increases with chain length while the preexponential remains relatively constant.<sup>53–55</sup> The present data show that the preexponential factor is greatest for ethanethiol and smallest for the longer chains. Indeed, hexanethiol, octanethiol, and decanethiol have approximately the same preexponential factor. While the preexponential factor should not be too greatly emphasized since it is notoriously difficult to measure, these data lead to the tentative conclusion that diffusion of the molecules across the surface is not likely to be responsible for this “bottleneck” to chemisorption. It seems more likely that orientation of the sulfur group with



respect to the surface is important and that shorter chain lengths such as ethanethiol have an advantage over the longer ones. However, this advantage is bound to saturate with increased chain length because of the increased chain flexibility. In this way the effect would become, for the longer chains, independent of chain length.

## 5. Conclusions

Alkanethiols physisorb to the surface of gold through van der Waals interactions that yield desorption enthalpies on the order of their bulk heats of vaporization. The molecules tend to bind more strongly to the gold surface than to each other in the bulk by a factor of about 1.15. This holds true for a wide variety of sulfur-containing alkanes of differing degrees of branching as well as thiophene. The physisorption enthalpy per  $\text{CH}_2$  group for alkanethiols is on the order of 6.1 kJ/mol, a value very similar to that observed for alkanes and 1-alkenes. The physisorption enthalpy contributed by the thiol group is on the order of 33 kJ/mol while the sulfur atom alone contributes  $\sim 24$  kJ/mol.

Alkanethiols show a chemisorption enthalpy of 126 kJ/mol, which is independent of chain length. This implies that, for chain lengths greater than 14 carbons, the physisorption enthalpy should be in fact higher than the chemisorption enthalpy. Indeed, longer thiols exhibit a single TPD feature at temperatures that are consistent with the projection of the physisorption enthalpy with chain length. The TPD spectra for thiols shorter than octanethiol show both a physisorption enthalpy and a chemisorption enthalpy. Octanethiol and longer chain thiols exhibit both the normal chemisorption feature and a higher energy peak at 148 kJ/mol. This higher energy peak can be annealed into the lower energy chemisorption peak. This is likely due to a rearrangement of the gold surface atoms which takes some time to occur and has an influence on the value of the S–Au surface bond. The lack of physisorption features for chain length longer than octanethiol is attributed to the fact that the chemisorption rate is large enough around 350 K that as the TPD temperature ramps through this region, if the molecules can remain physisorbed they rapidly become chemisorbed.

Sterically hindered thiol groups show less binding energy with the surface. Both *tert*-butanethiol and 2-propanethiol show physisorption enthalpies consistent with predictions based on an additive contribution to binding per methylene unit and a lower-than-normal chemisorption enthalpy of 107 kJ/mol. Adding one methylene group between the thiol and the *tert*-butyl group forms neopentanethiol. This species behaves “normally” in that it has a predicted physisorption enthalpy and a chemisorption enthalpy at 128 kJ/mol. The extra methylene group removes the steric hindrance of the *tert*-butyl group.

Diethyl sulfide and dibutyl sulfide both show only physisorption peaks. This is consistent with earlier studies of dialkyl sulfides on Au(111) that showed them to be poorly organized, physisorbed monolayers. Diethyl disulfide, however, showed only a chemisorption feature. This is consistent with Nuzzo's finding that the disulfide species tend to chemisorb more readily than the comparable thiols. Disulfides probably have a lower barrier to chemisorption due to the fact that they can chemisorb without the need to eliminate  $\text{H}_2$ .

By probing the rate of conversion from physisorbed layer to chemisorbed layer at 208 K for butanethiol and hexanethiol, it is found that the rate decreases from  $4 \times 10^{-4} \text{ s}^{-1}$  for butanethiol to  $3.3 \times 10^{-5} \text{ s}^{-1}$  for hexanethiol. These rates are similar to those found in constant exposure experiments that create a steady-state coverage of physisorbed molecules from which

chemisorption can occur. Arrhenius plots for ethanethiol, butanethiol, hexanethiol, and decanethiol adsorption rate indicate that the activation barrier to chemisorption for these molecules is about 29 kJ/mol irrespective of the chain length. This is consistent with a model involving a constant chemisorption well depth as the physisorption well depth increases with increased chain length. In this case the increased physisorption energy does not affect the height of the barrier but does increase the residence time of the molecules on the surface at temperatures where the chemisorption occurs more easily. The systematic study described in this paper has clarified several issues related to the adsorption of alkyl sulfides and other sulfur-containing molecules on Au(111) and has provided new clear challenges for those interested in the theoretical simulation of the behavior of this very popular system.

**Acknowledgment.** Support of the National Science Foundation (CHE-9619190, DMR-94-00362) and DOE (DE-FG02-93ER45503) for this research is gratefully acknowledged. We would also like to thank Paul Fenter, Peter Schwartz, and Arianne Eberhardt for helpful discussions.

## References and Notes

- (1) See references in: Atre, S. V.; Lieberg, B.; Allara, D. L. *Langmuir* **1995**, *11*, 3882.
- (2) Dubois, L. H.; Nuzzo, R. G. *Annu. Rev. Phys. Chem.* **1992**, *43*, 437.
- (3) Ford, J. F.; Vickers, T. J.; Mann, C. K.; Schlenoff, J. B. *Langmuir* **1996**, *12*, 1944.
- (4) Chailapakul, O.; Sun, L.; Xu, C.; Crooks, R. M. *J. Am. Chem. Soc.* **1993**, *115*, 12459.
- (5) DiMilla, P. A.; et al. *J. Am. Chem. Soc.* **1994**, *116*, 2225.
- (6) Dubois, L. H.; Zegarski, B. R.; Nuzzo, R. G. *J. Chem. Phys.* **1993**, *98*, 678.
- (7) Walczak, M. M.; Alves, C. A.; Lamp, B. D.; Porter, M. D. *J. Electroanal. Chem.* **1995**, *396*, 103.
- (8) Salem, L. *J. Chem. Phys.* **1962**, *37*, 2100.
- (9) (a) Thomas, R. C.; Sun, L.; Crooks, R. M.; Ricco, A. J. *Langmuir* **1991**, *7*, 620. (b) Buck, M.; Grunze, M.; Eisert, F.; Fisher, J.; Trager, F. *J. Vac. Sci. Technol. A* **1992**, *10*, 926.
- (10) Camillone III, N.; Leung, T. Y. B.; Scoles, G. *SPIE, OE/LASE Proc.* **1994**, 2125.
- (11) Gerlach, R.; Polanski, G.; Rubahn, H.-G. Submitted to *Appl. Phys. A*.
- (12) Poirier, G. E.; Pylant, E. D. *Science* **1996**, *272*, 1145.
- (13) Li, J.; Liang, K. S.; Camillone III, N.; Leung, T. Y. B.; Scoles, G. *J. Chem. Phys.* **1995**, *102*, 5019.
- (14) Schwartz, P. Manuscript in preparation.
- (15) Liu, G.-Y.; Song, X. *Langmuir* **1997**, *13*, 127.
- (16) Eberhardt, A.; Schwartz, P. Private communication.
- (17) Nuzzo, R. G.; Zegarski, B. R.; Dubois, L. H. *Am. Chem. Soc.* **1987**, *109*, 733.
- (18) Redhead, P. A. *Vacuum* **1962**, *12*, 203.
- (19) Poelsema, B.; Verheij, L. K.; Comsa, G. *Phys. Rev. Lett.* **1982**, *49*, 1731.
- (20) Bortolani, V.; Celli, V.; Franchini, A.; Idiodi, J.; Santoro, G.; Kern, K.; Poelsema, B.; Comsa, G. *Surf. Sci.* **1989**, *208*, 1.
- (21) Wetterer, S. M.; Lavrich, D. J.; Cummings, T.; Scoles, G.; Bernasek, S. To be submitted.
- (22) Dubois, L. H.; Zegarski, B. R.; Nuzzo, R. G. *J. Am. Chem. Soc.* **1990**, *112*, 570.
- (23) Sexton, B. A.; Hughes, A. E. *Surf. Sci.* **1984**, *140*, 227.
- (24) Nuzzo, R. G.; Dubois, L. H.; Allara, D. L. *J. Am. Chem. Soc.* **1990**, *112*, 558.
- (25) Nuzzo, R. G.; Fusco, F. A.; Allara, D. L. *J. Am. Chem. Soc.* **1987**, *109*, 2358.
- (26) Nishida, N.; Hara, M.; Sasabe, H.; Knoll, W. *Jpn. J. Appl. Phys.*, **1996**, *35*, 5866.
- (27) Sellers, H. *Surf. Sci.* **1993**, *294*, 99.
- (28) Feher, F. J.; Hemminger, J. C.; Dishner, M. H. *Langmuir* **1997**, *13*, 2318.
- (29) Lide, D. R. *Handbook of Chemistry and Physics*, 73rd ed.; CRC Press: London, 1992.
- (30) Fenter, P.; Eberhardt, A.; Eisenberger, P. *Science* **1994**, *266*, 1216.
- (31) Porter, M. D.; Zhong, C. J. *J. Am. Chem. Soc.* **1994**, *116*, 11616.

- (32) Troughton, E. B.; Bain, C. D.; Whitesides, G. M.; Nuzzo, R. G.; Allara, D. L.; Porter, M. D. *Langmuir* **1988**, *4*, 365.
- (33) Beulen, M. W. J.; Huisman, B.-H.; van der Heijden, P. A.; van Veggel, F. C. J. M.; Simons, M. G.; Biemond, E. M. E. F.; de Lange, P. J.; Reinhoudt, D. N. *Langmuir* **1996**, *12*, 6170.
- (34) Dishner, M. H.; Hemminger, J. C.; Feher, F. J. *Langmuir* **1996**, *12*, 6176.
- (35) Elfeninat, F.; Fredricksson, C.; Sacher, E.; Selmani, A. *J. Chem. Phys.* **1995**, *102*, 6153.
- (36) Izawa, M.; Kumihashi, T. *J. Chem. Phys.* **1995**, *103*, 9418.
- (37) Cassuto, A.; King, D. A. *Surf. Sci.* **1981**, *102*, 388.
- (38) Brivio, G. D.; Grimley, T. B. *Surf. Sci. Rep.* **1993**, *17*, 1.
- (39) Sullivan, D. J.; Flaum, H. C.; Kummel, A. C. *J. Phys. Chem.* **1993**, *97*, 12051.
- (40) Doren, D. J.; Tully, J. C. *J. Chem. Phys.* **1991**, *94*, 8428.
- (41) Rettner, C. T.; Mullins, C. B. *J. Chem. Phys.* **1991**, *94*, 1626.
- (42) Lee, C.-Y.; DePristo, A. E. *J. Chem. Phys.* **1986**, *85*, 4161.
- (43) Luntz, A. C.; Williams, M. D.; Bethune, D. S. *J. Chem. Phys.* **1988**, *89*, 4381.
- (44) D'Evelyn, M. P.; Steinruck, H.-P.; Madix, R. J. *Surf. Sci.* **1987**, *180*, 47.
- (45) D'Evelyn, M. P.; Hamza, A. V.; Gdowski, G. E.; Madix, R. J. *Surf. Sci.* **1986**, *167*, 451.
- (46) Rettner, C. T.; Scheizer, E. K.; Stein, H.; Auerbach, D. J. *J. Vac. Sci. Technol. A* **1989**, *7*, 1863.
- (47) Soulen, S. A.; Madix, R. J. *Surf. Sci.* **1995**, *323*, 1.
- (48) Hamza, A. V.; Steinruck, H.-P.; Madix, R. J. *J. Chem. Phys.* **1987**, *86*, 6506.
- (49) Kelley, D.; Weinberg, W. H. *J. Chem. Phys.* **1996**, *105*, 3789.
- (50) Mullins, C. B.; Weinberg, W. H. *J. Chem. Phys.* **1990**, *92*, 4508.
- (51) Mullins, C. B.; Weinberg, W. H. *J. Vac. Sci. Technol. A* **1990**, *8*, 2458.
- (52) Mullins, C. B.; Weinberg, W. H. In *Springer Series in Surface Sciences*, Madix, R. J., Ed.; Springer-Verlag: Berlin, 1994; Vol. 34 Surface Reactions.
- (53) Huang, D.; Chen, Y.; Fichthorn, K. A. *J. Chem. Phys.* **1994**, *101*, 11021.
- (54) Arena, M. V.; Deckert, A. A.; Brand, J. L.; George, S. M. *J. Phys. Chem.* **1990**, *94*, 6792.
- (55) Brand, J. L.; Arena, M. V.; Deckert, A. A.; George, S. M. *J. Chem. Phys.* **1990**, *92*, 5136.